Aalborg Universitet

Aalborg University
DENMARK

CFD Models of Persons Evaluated by Full-Scale Wind Channel Experiments

Brohus, Henrik; Nielsen, Peter V.

Publication date:
1996

Document Version
Publisher's PDF, also known as Version of record

AALBORG UNIVERSITY

DENMARK

CFD Models of Persons Evaluated by Full-Scale Wind Channel Experiments

Brohus, Henrik; Nielsen, Peter Vilhelm

Publication date:
1996

Citation for published version (APA):
Brohus, H., & Nielsen, P. V. (1996). CFD Models of Persons Evaluated by Full-Scale Wind Channel
Experiments. Aalborg: Dept. of Building Technology and Structural Engineering. (Indoor Environmental
Technology; No. 60, Vol. R9652).

INSTITUTTET FOR BYGNINGSTEKNIK
DEPT. OF BUILDING TECHNOLOGY AND STRUCTURAL ENGINEERING
AALBORG UNIVERSITET ● AAU ● AALBORG ● DANMARK

INDOOR ENVIRONMENTAL TECHNOLOGY
PAPER NO. 60

H. BROHUS & P. V. NIELSEN
CFD MODELS OF PERSONS EVALUATED BY FULL-SCALE WIND CHANNEL EXPERIMENTS

H. BROHUS & P. V. NIELSEN
CFD MODELS OF PERSONS EVALUATED BY FULL-SCALE WIND CHANNEL EXPERIMENTS

CFD MODELS OF PERSONS EVALUATED BY FULL-SCALE WIND CHANNEL EXPERIMENTS

Henrik Brohus
Assistant Professor
Aalborg University
Sohngaardsholmsvej 57
DK-9000 Aalborg
Denmark
Fax + 45 9814 8243
E-mail i6hb@civil.auc.dk

Peter V. Nielsen
Professor
Aalborg University
Sohngaardsholmsvej 57
DK-9000 Aalborg
Denmark
Fax + 45 9814 8243
E-mail i6pvn@civil.auc.dk

ABSTRACT

This paper presents three different CFD models of a person. The models are discussed and evaluated by comparison with full-scale measurements comprising a breathing thermal manikin standing in a wind channel. The three CFD models are made in a rectangular geometry. The most simple one is a heated cuboid with the same surface area and heat flux as a human being. The most complex one also includes "legs" and "head". The models are evaluated in a steady-state CFD simulation of personal exposure to a contaminant source in a uniform velocity field.

It is found that the models of a person are capable of simulating the important main features in the flow around a person. In all cases the simulated exposure approaches the same order of magnitude as the measured exposure. It is also found that inclusion of "legs" in the model might improve the result, especially when the contaminant source is located close to the floor.

KEY WORDS

Personal Exposure Assessment, CFD Model of Person, Breathing Thermal Manikin, Wind Channel Experiments.

1. INTRODUCTION

If we want to predict or control the personal exposure to a contaminant source in a ventilated room it is very important to take the local influence of the person itself into account. Numerous full-scale measurements have demonstrated that significant errors in personal exposure assessments may occur if this has not been considered (Rodes et al., 1991; Kim and Flynn, 1991; Brohus and Nielsen, 1994).

Errors exceeding one order of magnitude could easily be obtained (Brohus and Nielsen, 1995).

When Computational Fluid Dynamics (CFD) is used to predict the local airflow around a person and the personal exposure this raises the demand of a proper computational model of a person. With a sufficient degree of accuracy this model must be able to predict the important flow phenomena close to the person as well as the personal exposure and other parameters of interest. On the other hand it is necessary to keep track of the "economy" concerning the number of grid points, rate of convergence, CPU time, etc.

The optimum level of model complexity is highly case dependent. As

an example Davidson and Nielsen (1995) modelled the two-dimensional airflow in facial regions and nasal cavity to study the airflow close to the breathing zone. Others have modelled the whole person in a ventilated environment (Heinsohn, 1991; Gan, 1994; Murakami et al., 1995; Brohus and Nielsen, 1995) to include the interaction between the entire person and the flow field.

In this paper three different CFD models of a person are presented. They are all made in a rectangular geometry, ranging from a heated cuboid to a model including "legs" and "head". It has been the aim to propose models which are both able to re-create the characteristic flow phenomena observed close to a person, and at the same time they should be kept at a level of complexity that allows use in practical engineering purposes.

The models are compared to full-scale measurements performed in a wind channel using a breathing thermal manikin and a pollution source.

2. METHOD
2.1. CFD Models of a person
2.1.1. Geometry of models. In Figure 1 an outline of the three CFD models of a person is shown. Model 1 consists of a heated cuboid, Model 2 consists of one "torso" and two "legs" and finally, Model 3 which also includes a "head". The exact geometry is summarized in Table 1.

The height of the person and the surface area correspond to an average sized woman where the clothing has an insulation value of 0.8 clo. The convective heat flux of 25 W/m^2 corresponds to an activity level of a sedentary person or a person standing relaxed (~1 Met). The aspect ratio of the width and the depth for the models is kept approximately constant and equal to two.

Model 1   Model 2   Model 3
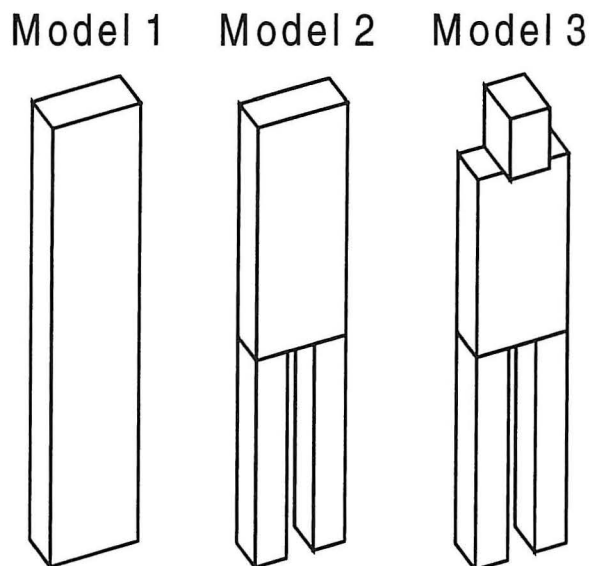
Figure 1. Outline of three different CFD models of a person made in a rectangular geometry.

TABLE 1. Geometry of three rectangular CFD models of a person.

PART	MODEL 1	MODEL 2	MODEL 3
Torso	1.7 x 0.3 x 0.16216	0.9 x 0.3 x 0.13803	0.67 x 0.3 x 0.14429
Leg	-	0.8 x 0.105 x 0.13803	0.8 x 0.105 x 0.14429
Head	-	-	0.23 x 0.13 x 0.18

Length x Width x Depth in metres.
Surface area: 1.62 m^2 (see note). Convective heat flux: 25 W/m^2.
NOTE: The surface area is the "exposed area", i.e. the part of the surface in contact with the surrounding air (this implies that the area in contact with the floor is not included).

One reason for choosing the specific dimensions, insulation value, etc. is to be able to make comparisons with the breathing themal manikin (see 2.2.1.).

2.1.2. Personal exposure. The personal exposure is defined as the concentration of inhaled contaminant. This is a convenient quantity with respect to the breathing thermal manikin where the respiration is simulated by an artificial lung. The above-mentioned CFD models, however, do not simulate the respiration directly. Therefore, the concentration of inhaled contaminant must be determined in another way. The inhaled pollution obviously comes from the contaminated air in the breathing zone close to the mouth and the nose. Comparisons were made between the pollution concentration in the nearest cell along the person at a height of 1.5 m above the floor and the mean concentration in a number of cells in a small volume around this point (~30 cm^3). The comparisons did not show any significant differences, consequently personal exposure was simulated as the contaminant concentration in the nearest cell along the person at the height of 1.5 m.

2.1.3. Governing equations. The governing equations describing the steady-state, three-dimensional flow field and the contaminant transport are: the continuity equation, the Navier-Stokes equations (velocity), the energy equation (temperature) and the concentration equation (contaminant transport). Turbulence was modelled by means of the two-equation k-ε model, where k is the turbulent kinetic energy, and ε is the dissipation rate of turbulent kinetic energy.

A rectangular grid is used with grid lines coinciding with the surfaces of the computational model of a person. The first grid line adjacent to the surface of the person is found at a distance of 1 cm, corresponding to a grid node distance of ½ cm from the surface. Standard wall functions were used to evaluate surface friction between the wall surfaces and the near-wall grid node. As mentioned in Table 1 a constant heat flux from the surface were prescribed. Due to the symmetry of the test case only one symmetry plane was simulated.

2.2. Full-scale measurements
2.2.1. Breathing Thermal Manikin. Full-scale measurements were performed by means of a Breathing Thermal Manikin (BTM) shown in Figure 2.
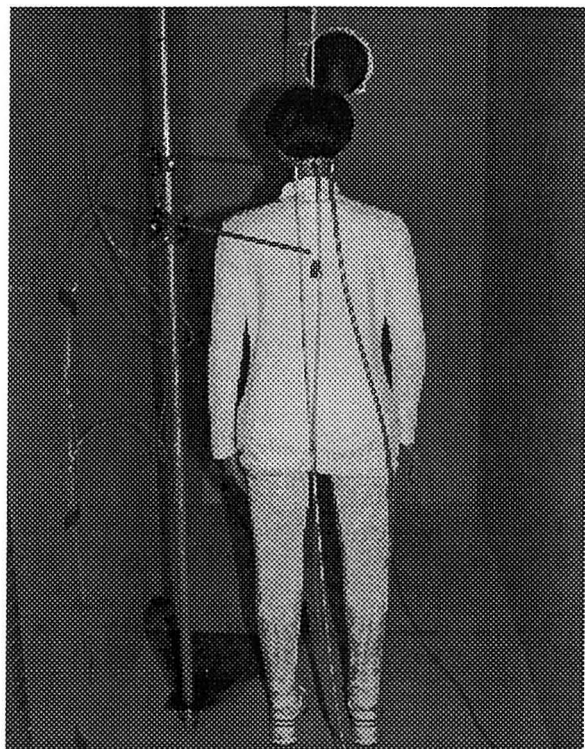

Figure 2. Breathing thermal manikin (used for the personal exposure measurements) standing in the full-scale wind channel. In the background of the photo one of the two exhaust openings is seen.

The BTM is shaped as a 1.7 m high average sized woman. The tight-fitting clothes have an insulation value of 0.8

clo. The manikin consists of a fibre armed polyester shell, wound with nickel wire used sequentially both for heating and for measuring and controlling the skin temperature. The heat output and the skin temperature are controlled to correspond to people in thermal comfort.

Respiration is simulated by an artificial lung.

2.2.2. Experimental setup. The measurements were performed in a wind channel (length x width x height = 2.44 m x 1.20 m x 2.46 m). The inlet opening was rounded to reduce turbulence generation. A uniform velocity field was created by extracting air through two exhaust openings in the one end. The amount of exhausted air was adjusted to obtain uniform velocity levels in the wind channel ranging from 0.05 m/s to 0.45 m/s. The air temperature was kept constant at approximately 21°C.

A contaminant source was simulated by tracer gas injected through a porous foam rubber ball, ø 0.1 m. The tracer gas was a neutral density mixture of nitrous oxide and helium.

3. RESULTS
3.1. The test case

In Figure 3 the test case is illustrated: a person facing a point contaminant source located at a horizontal distance of 0.5 m from the centre line of the person to the centre line of the source. At this fixed horizontal location, measurements and simulations were made with the contaminant source vertically located at five different heights above the floor (0.50 m, 0.75 m, 1.00 m, 1.25 m and 1.50 m).

The person was located in the uniform velocity field created in the wind channel. Here, the flow comes from behind the person through the opening in the one end and continues towards the two exhaust openings in the opposite

end. In front of the person a wake is created containing two large vertical vortices which have significant influence on the local airflow around the person and the transport of the contaminant (Brohus and Nielsen, 1995). Four different velocity levels were examined in the test case (0.05 m/s, 0.15 m/s, 0.30 m/s and 0.45 m/s).
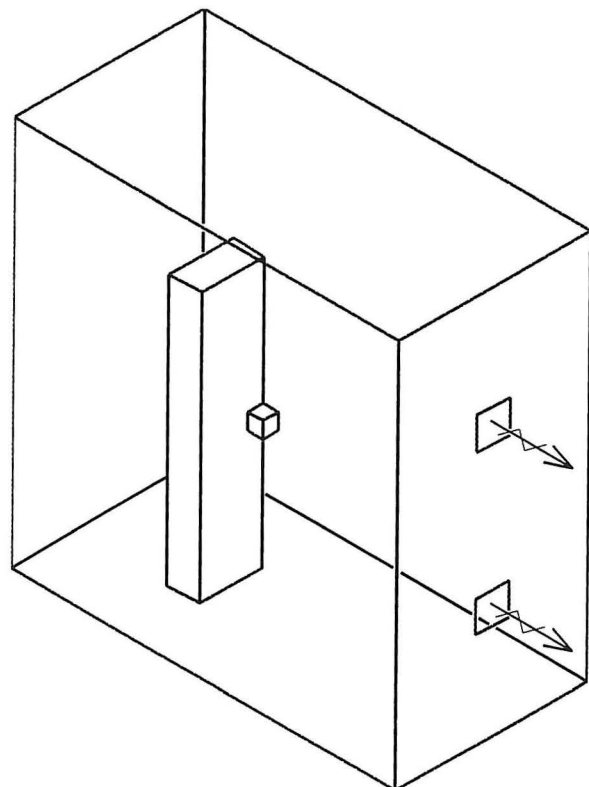
Figure 3. The test case: a person facing a contaminant source located in the uniform velocity field of a wind channel.

3.2. Computer simulations

Figure 4 shows two vector plots in the vertical symmetry plane for Model 1 and Model 3, respectively. Only a part of the velocity field is included in the figure. The fields are chosen to illustrate the complex flow field in front of the person and the influence of "legs" and "head".

Figure 5 illustrates the concentration distribution in the symmetry plane for two different vertical locations of the

contaminant source. The grey areas show where the local concentration exceeds the exhaust concentration more than 10 times. The velocity fields are the same as shown in Figure 4.

3.3. Personal exposure assessment

In Figure 6 results from measurements and simulations are presented. The figure shows the personal exposure as a function of the velocity level, and as a function of the vertical location of the contaminant source. Here, the personal exposure is made dimensionless by dividing by the contaminant concentration in the air exhausted from the wind channel. The curves are continuous interpolations based on the discrete

results from the simulations and the measurements.

4. DISCUSSION
4.1. Comparison between CFD models

The three CFD models of a person have all the same heat flux, height, surface area, and approximately the same aspect ratios. The differences are the inclusion of "legs" (Model 2) and "head" (Model 3) as seen in Figure 1.

The influence of the "legs" can easily be explored by looking at the flow fields in Figure 4 and at the different contaminant distributions in Figure 5.

In Figure 4 the flow field in the symmetry plane is shown. The vertical vortices created in the wake in front of the
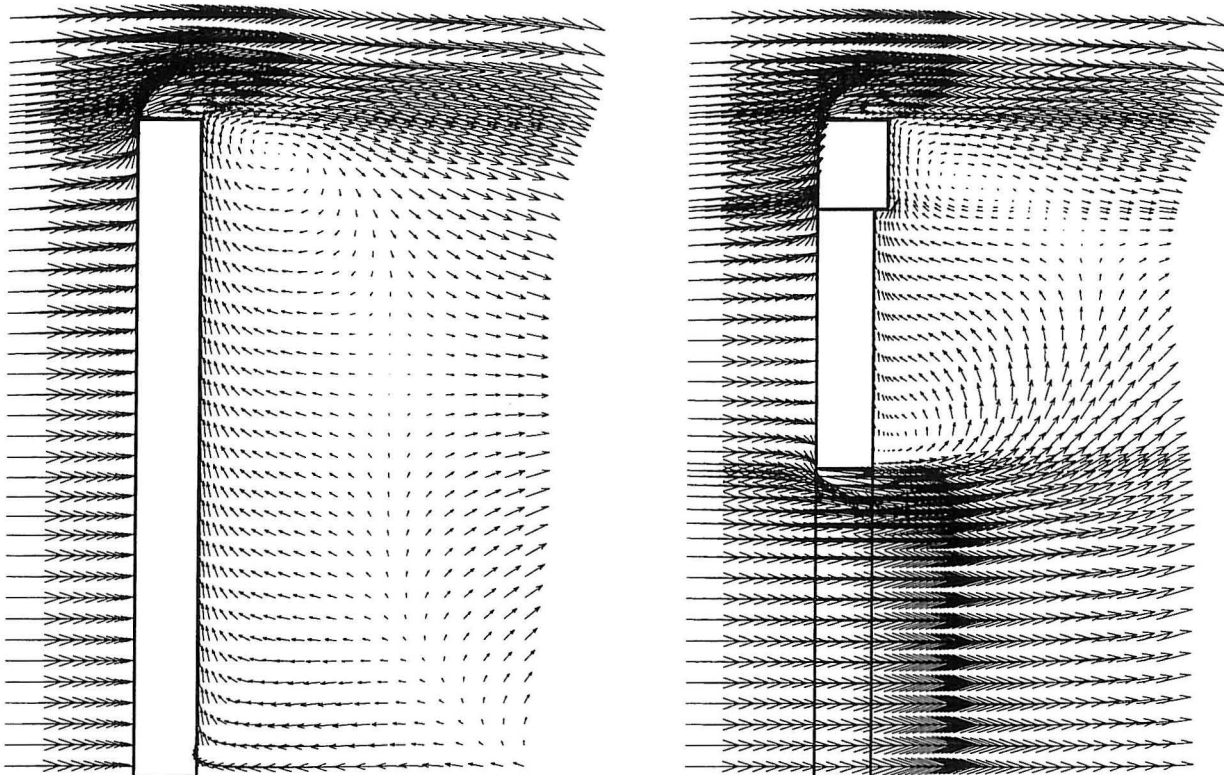

Figure 4. Simulated velocity field (part of) in the vertical symmetry plane of the wind channel for Model 1 (left) and for Model 3 (right). The uniform free stream velocity is 0.3 m/s.

5

person entrain air from a relatively high horizontal distance from the body and transport the air to the breathing zone. This entrainment takes place along the entire body using Model 1, while Model 3 only exerts the entrainment along the "torso". In the "leg" area the major differences are found: using Model 1 the flow is directed towards the person, while Model 3 causes a strong flow field in the opposite direction.

Figure 5 shows the influence of the differences concerning the contaminant transport and with it the personal exposure. Here, the grey areas show where the contaminant level exceeds the contaminant concentration in the exhaust air more than 10 times. For both models the concentration distribution indicates that the contaminant from the pollution source is entrained and transported to the breathing zone when the source is located 1.0 m above the floor. However, when the source is located only 0.5 m

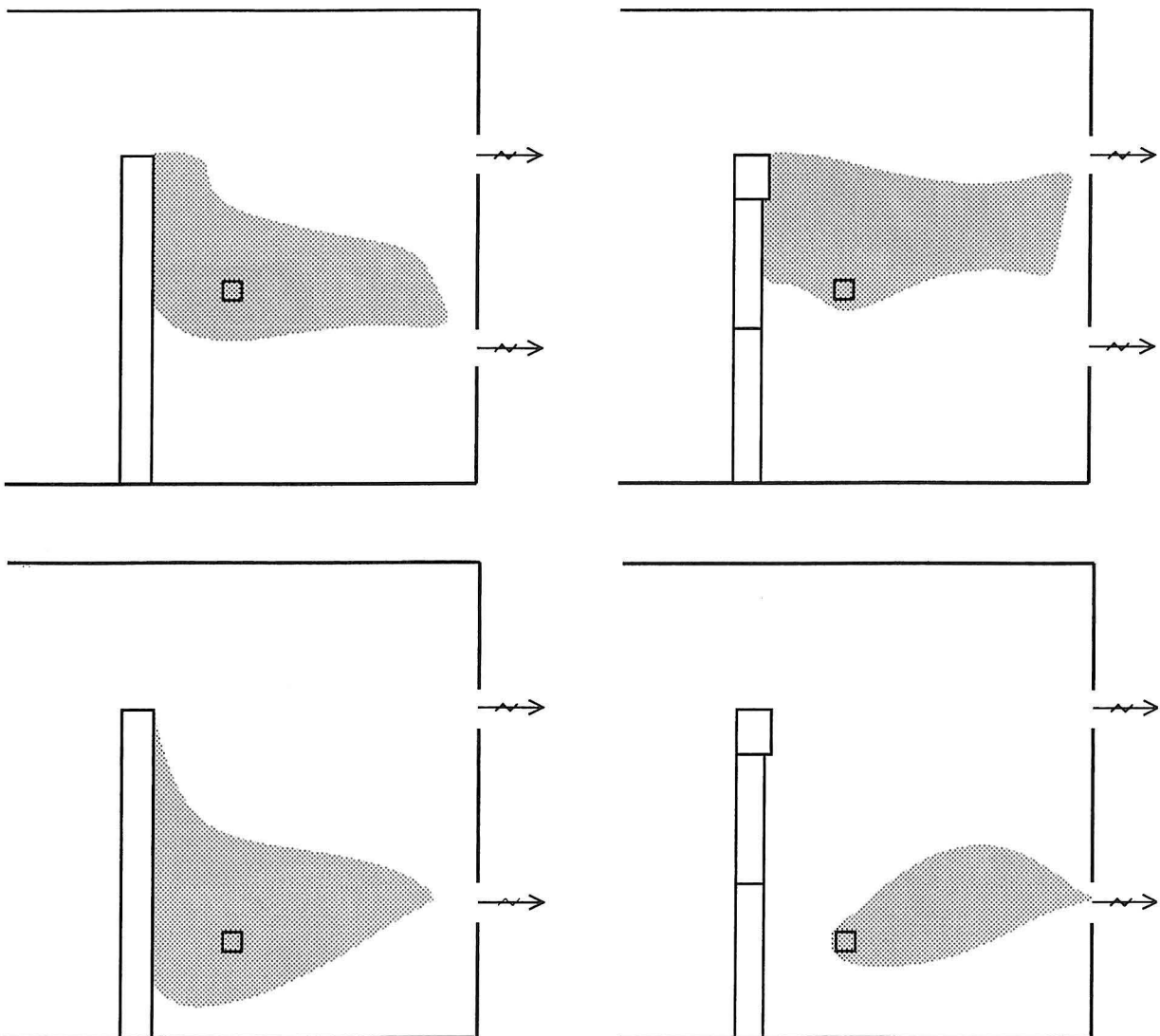**Figure 5.** Simulation of the concentration distribution in the vertical symmetry plane of the wind channel for Model 1 (left) and for Model 3 (right). Results for two different source locations are shown: 0.5 m above the floor (bottom) and 1.0 m above the floor (top). The grey areas show where the local concentration exceeds the exhaust concentration more than 10 times. The uniform free stream velocity is 0.3 m/s.

above the floor very different dispersion patterns are found. Model 1 causes entrainment and exposure, while Model 3 causes a removal of the pollution before it comes into contact with the person. As seen in Figure 6 this picture also apply for other source locations and velocity levels.

The behaviour of Model 2 versus Model 3 are found to be quite similar.

## 4.2. Comparison between measurements and simulations

Smoke visualizations in the wind channel have shown that the CFD models are capable of simulating important flow phenomena like the ascending boundary layer along the body, and the important wake region in front of the person, etc.

Figure 6 shows some differences in the prediction of personal exposure versus source location and free stream velocity. When the source is located near the floor and the velocity level is low both the BTM and Model 3 show no personal exposure, while significant exposure levels are obtained with Model 1. This reveals that inclusion of "legs" in a computational model of a person may be very important in certain cases.

The location of the maximum dimensionless exposure level is found for a source location between 1.00 m and 1.25 m above the floor in all cases, while the velocity level for maximum dimensionless exposure seems to be somewhat lower for the CFD models than for the BTM.

If the dimensionless exposure levels in Figure 6 are compared, a good correspondence is found between Model 1 and the BTM, while Model 3 seems to deviate with a factor of approximately two.

Figure 6 (right column). Dimensionless personal exposure to the contaminant source in the wind channel as a function of the source location and the free stream velocity.

7
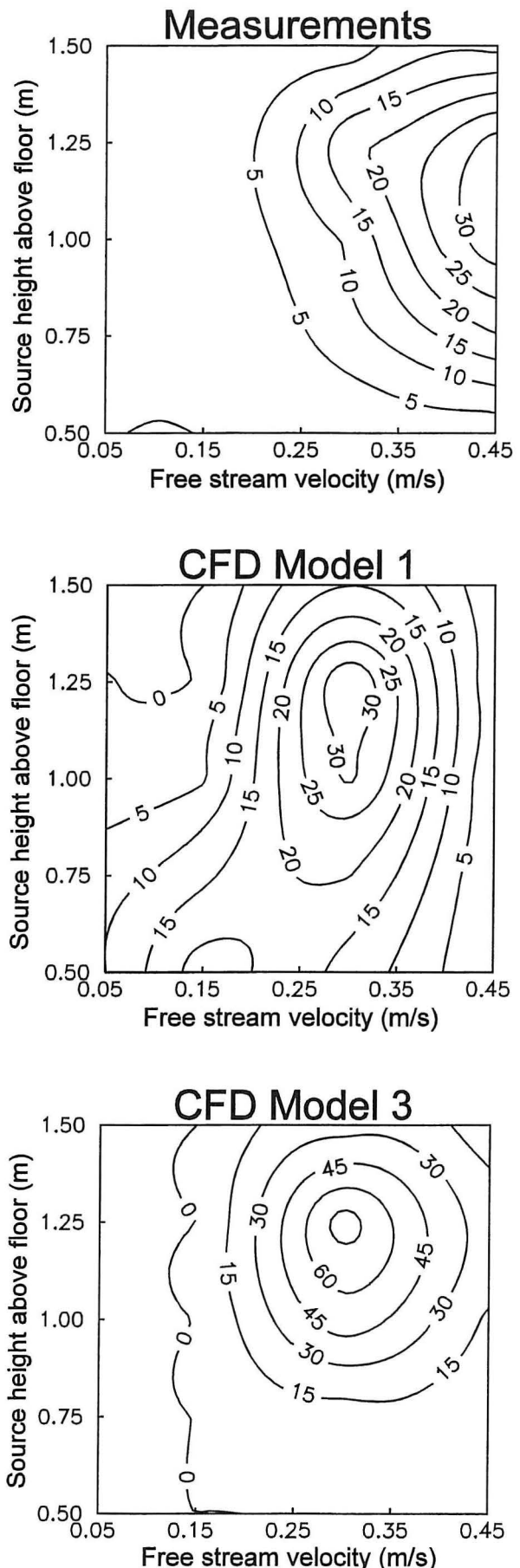
All the results, however, are found to be of the same order of magnitude, which is assumed to be a satisfactory result bearing the test case in mind. Here, the personal exposure of a person with a complex geometry in a three-dimensional flow field (subject to transient vortex shedding in the wake region) is modelled by a relatively simple rectangular steady-state CFD model.

The corresponding results for Model 2 (not included) show the same outline as Model 3, but with a generally lower exposure level, i.e. closer to the measurements.

If the results are compared with a simple "fully mixing" model (where the dimensionless personal exposure will be equal to one for all source locations and all velocity levels), we see that deviations exceeding a factor 30 or more may be obtained in this test case. This fact demonstrates the importance of taking the local influence of the person into account when the personal exposure is assessed.

5. CONCLUSIONS

Three different CFD models of a person are presented. The models are made in a rectangular geometry, and they range from a heated cuboid to a model including "legs" and "head". The models are discussed and evaluated by comparison with full-scale measurements comprising a breathing thermal manikin (BTM) standing in a wind channel.

It is found that the CFD models of a person are capable of simulating the important main features in the flow around a person. It is also found that inclusion of "legs" may be very important in certain cases. Comparison between the CFD models and the BTM shows that the simulated personal exposure approaches the same order of magnitude as the measured exposure.

ACKNOWLEDGEMENTS

REFERENCES

Brohus, H.; and P.V. Nielsen. 1994. Contaminant Distribution around Persons in Rooms Ventilated by Displacement Ventilation, Proc. of Roomvent '94, Fourth International Conference on Air Distribution in Rooms, Cracow, Poland, Vol. 1, pp. 293-312.

Brohus, H.; and P.V. Nielsen. 1995. Personal Exposure to Contaminant Sources in a Uniform Velocity Field, Proc. "Healthy Buildings '95", 4th International Conference on Healthy Buildings, Milano, Italy, Vol. 3, pp. 1555 - 1560.

Davidson, L.; and P.V. Nielsen. 1995. Calculation of the Two-Dimensional Airflow in Facial Regions and Nasal Cavity using an Unstructured Finite Volume Solver, ISSN 1395-7953 R9539, Dept. of Building Tech. and Struc. Engineering, Aalborg University, Denmark.

Gan, G. 1994. Numerical Method for a Full Assessment of Indoor Thermal Comfort, Indoor Air Journal, Vol.4, pp.154-168.

Heinsohn, R.J. 1991. Industrial Ventilation: Engineering Principles, ISBN 0-471-63703-3, New York, John Wiley & Sons.

Kim, T.; and Flynn, M.R. 1991. Airflow Pattern around a Worker in a Uniform Freestream, Am. Ind. Hyg. Assoc. Journal, 52(7), pp. 287-296.

Murakami, S.; S. Kato; and J. Zeng. 1995. Development of a Computational Thermal Manikin - CFD Analysis of Thermal Environment around Human Body, Proc. Tsinghua-HVAC-'95, Beijing, pp. 349-354.

Rodes, C.E.; R.M. Kamens; and R.W. Wiener. 1991. The Significance and Characteristics of the Personal Activity Cloud on Exposure Assessment Measurements for Indoor Contaminants, Indoor Air Journal, Vol.2., pp. 123-145.

PAPERS ON INDOOR ENVIRONMENTAL TECHNOLOGY

PAPER NO. 34: T. V. Jacobsen, P. V. Nielsen: *Numerical Modelling of Thermal Environment in a Displacement-Ventilated Room.* ISSN 0902-7513 R9337.

PAPER NO. 35: P. Heiselberg: *Draught Risk from Cold Vertical Surfaces.* ISSN 0902-7513 R9338.

PAPER NO. 36: P. V. Nielsen: *Model Experiments for the Determination of Airflow in Large Spaces.* ISSN 0902-7513 R9339.

PAPER NO. 37: K. Svidt: *Numerical Prediction of Buoyant Air Flow in Livestock Buildings.* ISSN 0902-7513 R9351.

PAPER NO. 38: K. Svidt: *Investigation of Inlet Boundary Conditions Numerical Prediction of Air Flow in Livestock Buildings.* ISSN 0902-7513 R9407.

PAPER NO. 39: C. E. Hyldgaard: *Humans as a Source of Heat and Air Pollution.* ISSN 0902-7513 R9414.

PAPER NO. 40: H. Brohus, P. V. Nielsen: *Contaminant Distribution around Persons in Rooms Ventilated by Displacement Ventilation.* ISSN 0902-7513 R9415.

PAPER NO. 41: P. V. Nielsen: *Air Distribution in Rooms - Research and Design Methods.* ISSN 0902-7513 R9416.

PAPER NO. 42: H. Overby: *Measurement and Calculation of Vertical Temperature Gradients in Rooms with Convective Flows.* ISSN 0902-7513 R9417.

PAPER NO. 43: H. Brohus, P. V. Nielsen: *Personal Exposure in a Ventilated Room with Concentration Gradients.* ISSN 0902-7513 R9424.

PAPER NO. 44: P. Heiselberg: *Interaction between Flow Elements in Large Enclosures.* ISSN 0902-7513 R9427.

PAPER NO. 45: P. V. Nielsen: *Prospects for Computational Fluid Dynamics in Room Air Contaminant Control.* ISSN 0902-7513 R9446.

PAPER NO. 46: P. Heiselberg, H. Overby, & E. Bjørn: *The Effect of Obstacles on the Boundary Layer Flow at a Vertical Surface.* ISSN 0902-7513 R9454.

PAPER NO. 47: U. Madsen, G. Aubertin, N. O. Breum, J. R. Fontaine & P. V. Nielsen: *Tracer Gas Technique versus a Control Box Method for Estimating Direct Capture Efficiency of Exhaust Systems.* ISSN 0902-7513 R9457.

PAPER NO. 48: Peter V. Nielsen: *Vertical Temperature Distribution in a Room with Displacement Ventilation.* ISSN 0902-7513 R9509.

PAPER NO. 49: Kjeld Svidt & Per Heiselberg: *CFD Calculations of the Air Flow along a Cold Vertical Wall with an Obstacle.* ISSN 0902-7513 R9510.

PAPER NO. 50: Gunnar P. Jensen & Peter V. Nielsen: *Transfer of Emission Test Data from Small Scale to Full Scale.* ISSN 1395-7953 R9537.

PAPER NO. 51: Peter V. Nielsen: *Healthy Buildings and Air Distribution in Rooms.* ISSN 1395-7953 R9538.

PAPERS ON INDOOR ENVIRONMENTAL TECHNOLOGY

PAPER NO. 52: Lars Davidson & Peter V. Nielsen: *Calculation of the Two-Dimensional Airflow in Facial Regions and Nasal Cavity using an Unstructured Finite Volume Solver.* ISSN 1395-7953 R9539.

PAPER NO. 53: Henrik Brohus & Peter V. Nielsen: *Personal Exposure to Contaminant Sources in a Uniform Velocity Field.* ISSN 1395-7953 R9540.

PAPER NO. 54: Erik Bjørn & Peter V. Nielsen: *Merging Thermal Plumes in the Indoor Environment.* ISSN 1395-7953 R9541.

PAPER NO. 55: K. Svidt, P. Heiselberg & O. J. Hendriksen: *Natural Ventilation in Atria - A Case Study.* ISSN 1395-7953 R9647.

PAPER NO. 56: K. Svidt & B. Bjerg: *Computer Prediction of Air Quality in Livestock Buildings.* ISSN 1395-7953 R9648.

PAPER NO. 57: J. R. Nielsen, P. V. Nielsen & K. Svidt: *Obstacles in the Occupied Zone of a Room with Mixing Ventilation.* ISSN 1395-7953 R9649.

PAPER NO. 58: C. Topp & P. Heiselberg: *Obstacles, an Energy-Efficient Method to Reduce Downdraught from Large Glazed Surfaces.* ISSN 1395-7953 R9650.

PAPER NO. 59: L. Davidson & P. V. Nielsen: *Large Eddy Simulations of the Flow in a Three-Dimensional Ventilated Room.* ISSN 1395-7953 R9651.

PAPER NO. 60: H. Brohus & P. V. Nielsen: *CFD Models of Persons Evaluated by Full-Scale Wind Channel Experiments.* ISSN 1395-7953 R9652.

PAPER NO. 61: H. Brohus, H. N. Knudsen, P. V. Nielsen, G. Clausen & P. O. Fanger: *Perceived Air Quality in a Displacement Ventilated Room.* ISSN 1395-7953 R9653.

PAPER NO. 62: P. Heiselberg, H. Overby & E. Bjørn: *Energy-Efficient Measures to Avoid Downdraft from Large Glazed Facades.* ISSN 1395-7953 R9654.

PAPER NO. 63: O. J. Hendriksen, C. E. Madsen, P. Heiselberg & K. Svidt: *Indoor Climate of Large Glazed Spaces.* ISSN 1395-7953 R9655.

PAPER NO. 64: P. Heiselberg: *Analysis and Prediction Techniques.* ISSN 1395-7953 R9656.

PAPER NO. 65: P. Heiselberg & P. V. Nielsen: *Flow Element Models.* ISSN 1395-7953 R9657.

PAPER NO. 66: Erik Bjørn & P. V. Nielsen: *Exposure due to Interacting Air Flows between Two Persons.* ISSN 1395-7953 R9658.

PAPER NO. 67: P. V. Nielsen: *Temperature Distribution in a Displacement Ventilated Room.* ISSN 1395-7953 R9659.

PAPER NO. 68: G. Zhang, J. C. Bennetsen, B. Bjerg & K. Svidt: *Analysis of Air Movement Measured in a Ventilated Enclosure.* ISSN 139995-7953 R9660.